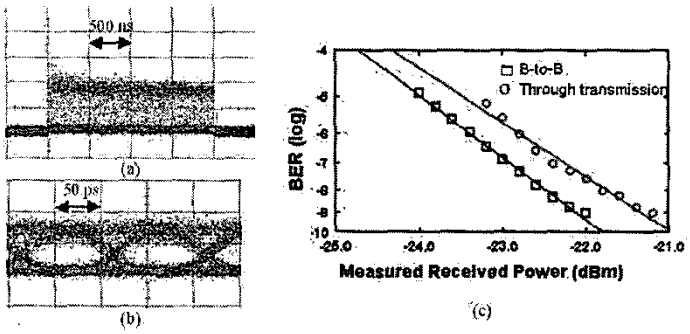

Fig. 4: a) Waveform of the 2-us data burst sent from the slave node and received at the master node, b) A zoom-in eye diagram of the 10-Gb/s signal, c) BER measurements.

two nodes are connected to the AWG to demonstrate the master/slave type of synchronization. Between the network nodes and the AWG, they are interconnected by conventional single mode fibers (SMFs). The fiber lengths used for node 1 and 2 are 8 km and 1 km, respectively.

In node 1 that plays the master role, the MFL outputs two wavelengths at 1553.3 nm and 1558.2 nm, respectively. At these two wavelengths, SNYC frames with the same pattern are generated by directly modulating the MFL. The inset in the figure shows the simultaneous two-wavelength signal output. The SYNC frame would contain flags, synchronization information and control field. However for this particular proof-of-concept demonstration, the SYNC frame is CW with duration of 200 ns to simplify data processing at the receiving ends. Therefore, in node 2 that is the slave node in the experiment, the receiver only detects the power of the quasi-CW light. The receiver output triggers a delay circuit. The circuit generates $2D_1$ - $2D_2$ time delay, where D_1 corresponds to 8 km and D_2 corresponds to 1 km, respectively. The delayed trigger signal then initiates a tunable transmitter to send data to node 1 by tuning the wavelength accordingly.

Fig. 4a shows at node 1 the observed waveform of a data burst sent from the slave node. Node 2 is synchronized with node 1 by checking the delay circuit output and the master clock together using an oscilloscope. The SYNC frames are broadcast periodically. Node 2 generates 10-Gb/s data burst with 2us-duration upon receiving of the trigger signal from the delay circuit. A zoom-in eye diagram is also provided in Fig. 4b. The data is generated from continuous pseudo-random bit sequence (PRBS) having a word length of 2^{31}-1. The data burst is obtained by chopping the PRBS to 2-us length. The BER measurement is performed by gating the BER tester following the receiver in the master node. Fig. 4c shows the BER measurements, less than 1-dB penalty is observed through the AWG and after transmission. The penalty is possibly caused by the power transient of the packets.

4. Conclusion

We present a simple synchronization scheme for wavelength-routed star networks based on broadcasting frames from a MFL. The scheme does not rely on out-of-band signaling or optical delay lines, therefore it reduces the hardware cost and simplifies the system design.

References:

[1] R. Theodore Hofmeister, Chung-Li Lu, Min-Chen Ho, Pierluigi Poggiolini, and Leonid G. Kazovsky, "Distributed slot synchronization (DSS): A network-wide slot synchronization technique for packet-switched optical networks." *J. Lightwave Technol.*, Vol. 16, No. 12, 1998, pp. 2109-2116.

[2] Takashi Sakamoto, Akira Okada, Mamoru Hirayama, Yoshihisa Sakai, Osamu Moriwaki, Ikuo Ogawa, Rieko Sato, Kazuto Noguchi, and Morito Matsuoka, "Optical packet synchronizer using wavelength and space switching." *IEEE Photon. Technol. Lett.*, Vol 14, No. 9, 2002, pp. 1360-1362.

[3] M. Kauer, M. Girault, J. Leuthold, J. Honthaas, O. Pellegri, C. Goullancourt, and M. Zirngibl, "16-channel digitally tunable packet switching transmitter with sub-nanosecond switching time." in *Proc. ECOC 2002*, paper 3.3.3.

[4] P. P. Iannone, K. C. Reichmann, and N. J. Frigo, "High-speed point-to-point and multiple broadcast services delivered over a WDM passive optical network." *IEEE Photo. Technol. Lett.*, Vol. 10, No. 9, 1998, pp. 1328-1330.

MF105 **5:30 PM**

An All-Optical Bufferless Multiwavelength Sorter for 40 Gb/s Asynchronous Variable-Length Optical Packets

Z. Hu, S. Rangarajan, L. Rau, D. Blumenthal, *Optical Communications and Photonic Networks Group, Department of Electrical and Computer Engineering, University of California, Santa Barbara, Santa Barbara, CA, Email: huby@ece.ucsb.edu.*

We present a new all-optical multiwavelength sorter designed for asynchronous, variable-length packets. We demonstrate experimentally that the scheme efficiently implements sorting function without contention for 40 Gb/s variable packets at a BER of less than 10^{-9} without an error floor.

1. Introduction

Packet switched optical networks require methods to handle contention when multiple packets compete for the same resources at e.g. switch output ports. However, there has not been an efficient contention resolution technique to handle contention between Internet Protocol (IP) packets that are inherently variable in length and arrive at a switch asynchronously with respect to each other [1][2].

In this paper we present a new unbuffered multi-wavelength sorter (multi-λ sorter) that supports very high bit-rate, variable-length packets arriving asynchronously. We demonstrate experimentally that the scheme can implement sorting function without contention at error free operation between multiple input-ports asynchronously loaded with 40Gb/s variable-length packets. To the best of our knowledge, this is the first time an all-optical sorter for asynchronous and variable length packets has been demonstrated. The multi-λ sorter, which is based on the 2x2 λ-contention resolution switch (λ-switch) constructed from latching optical cross-coupled λ-decision circuits, converts incoming packets to new wavelengths (λ_1, λ_2 ,...,λ_n) according to the order of arrival time. The packets are re-ordered at the output ports according to wavelength dependent priority without contention. The sorter is inherently latching and maintains packet switching state for the whole duration of the packet or overlapping contending packets, without fragmentation while enabling operation with any length packet arriving asynchronously at multiple input ports.

2. Principle of Operation

The architecture of the all-optical multi-λ sorter is shown schematically in Figure 1 can be used as front end to an optical switch stage. The packet sorter is a multi-stage asynchronous switch consisting of multiple 2x2 λ-contention resolution switches. The function of sorter is to sort the incoming packets on original wavelength λ_s so that first-in packets arrive at the top outputs with λ_1 and last in packets at the bottom outputs with λ_n. The 2x2 λ-contention resolution switches operate asynchronously and are latching so that packets that arrive first or overlapping packets arriving in the 2x2 λ-contention resolution switch at the same time, will be completely switched to the correct port without fragmentation. All packets with different wavelengths are switched simultaneously to desired links using an optical switch. Variable-length packets $P^{(m)}{}_n$ where packet 'n' arrives at the input port 'm': $P^{(1)}{}_1$, $P^{(1)}{}_2$, ..., $P^{(1)}{}_n$and $P^{(2)}{}_1$, ..., $P^{(2)}{}_n$, ..., and $P^{(n)}{}_1$,..., and $P^{(n)}{}_n$, arrive asynchronously at the input-ports on λ_s. Increasing length fiber delay lines are used to provide fixed processing time delays between switches. $P^{(1)}{}_1$ and $P^{(2)}{}_1$ are processed by the first 2x2 λ-switch (S_1) according to the following rule: (i) if $P^{(1)}{}_1$ arrives first it is converted to λ_1 and $P^{(2)}{}_1$ is converted to λ_2; (ii) if $P^{(2)}{}_1$ arrives first it is converted to λ_1 and $P^{(1)}{}_1$ to λ_2; (iii) when any one of two packets is absent, the switch outputs a packet with λ_1. Considering possible case that $P^{(3)}{}_1$comes first among $P^{(1)}{}_1$, $P^{(2)}{}_1$ and $P^{(3)}{}_1$, second (S_2) and third 2×2 λ-switches (S_3) are used to further process $P^{(3)}{}_1$, $P^{(2)}{}_1$ and $P^{(1)}{}_1$ then assign λ_1, λ_2 and λ_3 to them according to the same above rules. This process continues for $P^{(4)}{}_1$, $P^{(5)}{}_1$,..., and $P^{(n)}{}_1$ until all packets are sorted at the first stage according to the rule described above. In order to handle all *n* incoming packets, n(n-1)/2 cascaded 2x2 λ-contention resoltuion switches need to be used.

It is important to emphasize the mechanism by which asynchronous, variable-length packet are switched using the latching function in order to keep the λ-contention resoltuion switches in a fixed state until the longest packet and all overlapping shorter packets at both inputs have exited the switch. The state of the switch is then reset and will set its new state based on the next packet arrival at its input-ports once both ports are clean for a certain time (i.e., switching time). An additional feature of this design is that a packet can be erased at any time by turning off the corresponding wavelength. These two features, reading and erasure of packets are important to allow priority queuing for applications where a variety of differentiated services are carried by the packets (e.g. voice, video).

The 2x2 λ-contention resolution switch is shown in Figure 2(a). Packets entering input-port 1 and input-port 2 namely, $P^{(1)}$ and $P^{(2)}$ are fed to the switch. The packet λ-decision blocks generate the desired probe CW signal to wavelength converters based on the priority of the incoming packets. The probe signals of the packet λ-decision blocks are generated by cross coupled probe signal circuits for each λ as shown in the inset of Figure 2(a). The packet streams $P^{(1)}$ and $P^{(2)}$ serve as input parameters for the λ probe control circuit. Setting one probe signal automatically resets the other λ probe signal to prevent transmission of the packet on both the priority channels, thereby making the λ probe control signals mutually exclusive. Figure 3 shows the physical implementation details that provide the logic for the probe control circuit. The output probe signal, generated on a per packet basis is then fed to a wavelength converter along with the corresponding data line to switch the packet to the desired priority access port. Figure 2(b) shows the timing diagram for the signals generated for the different cases of possible incoming variable and asynchronous packets in particular reference to $P^{(2)}$ packet λ- decision block detailed in the inset.

3. Experiment Setup and Results

The experimental setup for demonstrating operation of $P^{(2)}$ packet λ-decision in a 2×2 contention resolution switch is shown in Figure 3. A 10GHz fiber ring laser is used to generate pulses at 1555nm (λ_s). Its output was modulated with a variable length (PRBS 2^{31}-1) packet source (BERT), and then multiplexed from 10Gb/s to 40Gb/s. To demonstrate asynchronous and variable length packets, the 40Gb/s data output was split into two parts by a splitter: one part was regarded as input packets of $P^{(2)}_1$, ...,$P^{(2)}_n$ at input-port 1and the other part went through a fiber spool (~11.2μs delay) as packets of $P^{(1)}_1$, $P^{(1)}_2$, ...,$P^{(n)}_1$ at input-port 2. Considering the delay time of the fiber spool, we generated four packet lengths, 4.7μs, 4.5μs, 4.7μs and 4.9μs in duration and interval time is 0.8μs, which is shown as the inset waveform in Figure 3.

In the first experiment, we demonstrated that λ_2 optical probe signal was produced basing on packet arrival sequence at input-port 2. The probe circuit consists of two parts: one part is constructed from CW fiber ring laser structure. When packets present, packets suppressed the lasing in the CW ring laser; the other part is a cross gain modulation (XGM) function to invert the CW ring laser output signal to the same polarity as the existence of packets using another SOA. A new wavelength 1547nm (λ_2) was simultaneously issued during this processing step.

We used an acousto-optical modulator (AOM) to simulate λ_1 optical probe signal. The signal from AOM has the wavelength 1558nm λ_1) and was split into two parts: one part feedbacks to control the λ_2 probe signal; the other part was delayed to combine with λ_2 probe signal to form desired $\lambda_1+\lambda_2$ probe signal as the input probe signal for wavelength conversion of the packets at input-port 2. Corresponding timing diagram was recorded as shown as the inset waveform in Figure 3. Then, the $\lambda_1+\lambda_2$ probe signal was coupled with the packets at input-port 2 to enter a fiber wavelength converter [3]. As shown as the inset waveform in Figure 3, three wavelengths are present simultaneously in the input signal for the wavelength converter, which are λ_s:1555nm, λ_1:1558nm, λ_2:1547nm, respectively.

In the second experiment, we demonstrated that the packets at input-port 2 (data signal) were converted from λ_s to λ_1 or λ_2 depending on the different arrival time, which is shown as the inset waveform in Figure 3. The corresponding eye diagrams are clean and open well. Since λ_1 part of the output packets was directly produced by AOM (simulation signal), only BER of λ_2 part was measured and plotted as a function of the received optical power, which is also shown in Figure 3. The dashed lines are the BER curves for back-to-back (BTB) and the solid lines are the BER curves for λ_2 (1547nm) part of output packets. The maximum power penalty for any channel is less than 3-dB at BER of 10^{-9} compared with the input packets. The power penalty was mainly caused by the relatively low optical probe signals.

4. Summary and Conclusion

We have presented a new all-optical bufferless multiwavelength sorter for asynchronous variable length packets without contention. BER results show that it is error free operation for 40Gb/s variable length packets. The maximum power penalty for any channel is less than 3-dB compared with back-to-back. The priority strategy used in the multi-λ sorter can easily be modified to accommodate other schemes.

Acknowledgements

The authors gratefully thank Paul Donner and Russ Gyurek from Cisco System for useful discussions.

References

[1] J. P. Lang, E. A. Varvarigos, D. J. Blumenthal, J. of Lightwave Technol., Vol. 18, pp. 1049, 2000.
[2] L. Tancevski, S. et. al., IEEE J. Select. Areas Commun., Vol. 18, pp. 2084-2093, 2000.

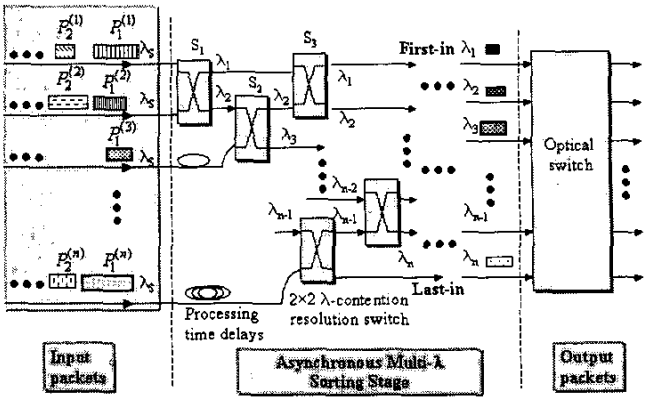

Fig. 1 Proposed all-optical sorting scheme for multiple packets

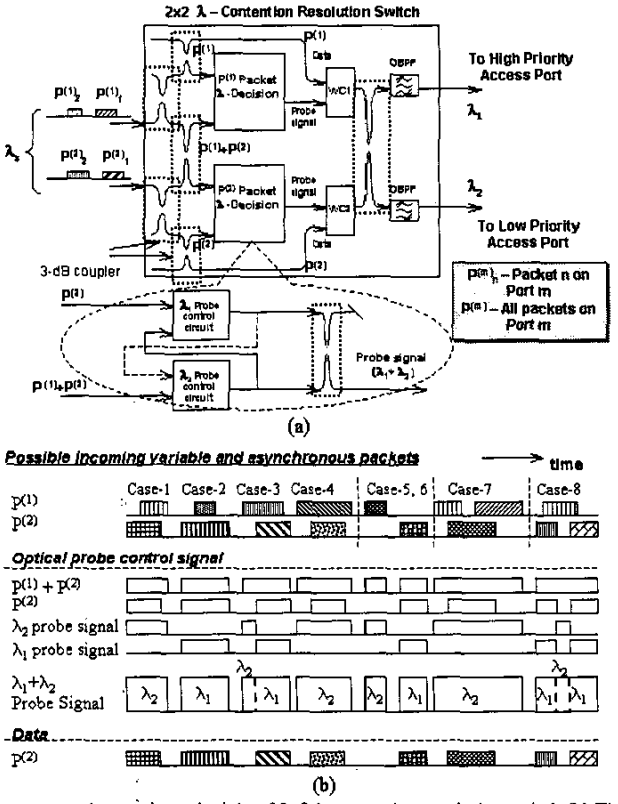

Fig. 2 (a) Structure and operation principle of 2×2 λ-contention resolution switch (b) Timing diagram for probe signals generated

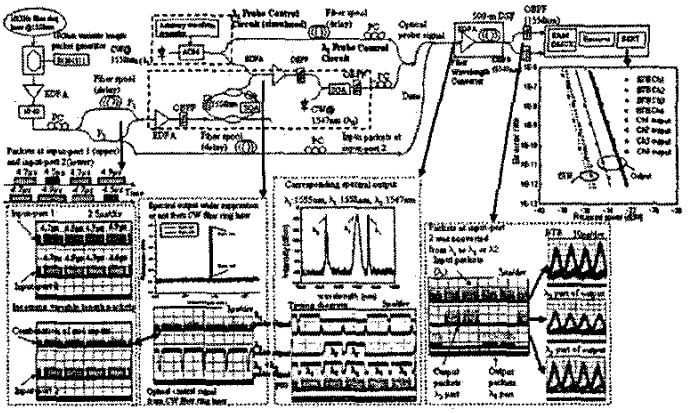

Fig. 3 Experimental setup. MOD: Modulator. PC: Polarization Controller. OBPF: Optical Bandwidth-pass Filter

[3] B. E. Olsson; P. Ohlen; L. Rau, D. J. Blumenthal, IEEE Photon. Technol. Lett., Vol. 12, pp. 846-848, 2000.

MF106 **5:30 PM**

Pre-Deployment of OEOs in Agile Photonic Networks

O. Gerstel, ONG, Cisco System, San Jose, CA; H. Raza, Transparent Networks, San Jose, CA, Email: ori@ieee.org.

We show that the main capital cost for remote configurability in optical networks lies in how OEO resources must be pre-deployed in preparation for the next connection request. Photonic switches reduce this cost significantly compared to electrical switches.

1. Introduction

Optical networks are expected to become remotely configurable (also termed "agile") in the near future. This capability will reduce the operational expenses (OPEX) of dispatching craftspeople to remote sites for manually configuring connections. It will also reduce the time for setting up new services, thereby preventing delays in revenues for new services or even loss of customers to competing carriers. Once connection setup times are in the order of minutes to seconds, network agility will also enable new types of services at the photonic layer, such as bandwidth on demand and automated photonic restoration.

At the same time, network agility does not come for free. Today's photonic networks are typically based on fixed photonic components that cannot tune to support a different connection configuration. Introducing tunable components will somewhat increase the cost of the solution [1]. Even more importantly, such automation means that the relevant resources to support the next connection request must be in place before hand and thus the cost of the network must always be higher than the absolute minimum needed for the current level of traffic. This phenomenon is called "pre-deployment" of resources (or "over-provisioning"). Since photonic layer resources - in particular transponders and regenerators (termed OEOs herein) - are expensive, network agility has a capital expense (CAPEX) implication that to some degree offsets the above OPEX advantages.

We believe that the extent of network agility represents one of the key dilemmas carriers will be facing in coming years, as they struggle to reduce both CAPEX and OPEX.

While most of the research on agile optical networking has been focusing on the control plane of the network (e.g., [2]), very little has been done on how to size the physical network for such dynamism (e.g., [3]), and we are not aware of any work that takes into account the required pre-deployment of hardware to this end. This is the focus of our paper.

2. Architectures for photonic network agility

The architectures for network agility at the optical transport layer can be broadly classified into two major categories:

(a) Agile electrical overlay: a static photonic layer with an agile electrical overlay layer, using EXCs supports the benefits of photonic bypass while avoiding photonic switching. Note that the use of EXCs does not imply that the network is fully opaque, as shown in Fig. 1(a) vs. Fig. 1(b). In such networks, lightpaths are manually deployed between EXCs at remote sites during network setup and OEOs (standalone or integrated) terminate these lightpaths into the EXC. During normal operation, the EXCs switch traffic between these lightpaths without manual intervention.

(b) Agile photonic layer: In this case, agility is provided through photonic switching elements, which maintain the signal in the optical domain. For the purposes of this discussion, it does not matter what technology is used for photonic switching, as long as it provides full flexibility. We use the term PXCs to represent this function. Such a PXC allows full access to the line capacity by dynamically connecting any OEO resource

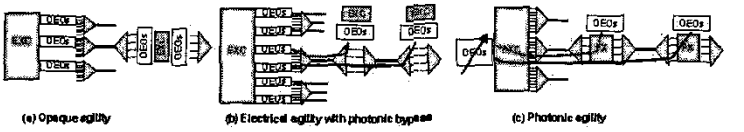

Figure 1: Architectures for the agile optical transport layer

onto any wavelength on the line, as shown in Fig. 1(c), where the same OEO can be used to connect to different remote sites depending on the current demands.

3. Cost of network agility

Any agile solution requires pre-deployment of enough resources to support future traffic demands until the next time craftspeople are dispatched to the site. In the photonic network case, the predominant cost of pre-deployment is associated with OEOs due to their relative high cost versus the cost of the line systems and due to the fact that the line systems typically (but not always) have enough spare wavelengths to support additional traffic while OEOs are deployed on a per-connection basis. In an ideal world, where traffic forecasts are accurate, the sizing of the network for the next deployment cycle (say, the next year) includes routing of the forecasted demands and using this information to determine how many resources are needed in a particular direction out of a node to support the forecast. In this case, there is no waste in resources over a manual network, in which resources are deployed when traffic demands materialize. However, in reality traffic forecasts are inaccurate. As a result, the pre-deployed resources are not always positioned in the right place for the traffic. This leaves the carrier with three choices: (1) design the network to support variations of the forecasted traffic pattern; (2) set up a sub-optimal route for the traffic using existing resources; or (3) send craftspeople to put the right resources in as needed. Assuming traffic demands have to be quickly satisfied, the third alternative is not viable. The second alternative creates long-term inefficiencies in the network since carriers' are reluctant to later optimize their network.

Inaccurate traffic forecasts are handled better if the photonic layer is agile, as opposed to electrical agility. In opaque networks (Fig. 1(a)) electrical agility requires forecasts on a per-link basis, since one has to connect OEOs in the right direction out of a node. Thus forecasts have to be accurate down to the link level. The problem is exacerbated in networks where electrical agility is coupled with non-agile photonic bypass (Fig. 1(b)), since the OEOs have to be connected to the right photonic adjacency, not just to the right link. Thus if one lightpath connects the 1st node to the 2nd node and another lightpath connects the 1st node to the 3rd node with photonic bypass at the 2nd node (as shown in the figure), two OEOs have to be pre-deployed to allow flexibility to reach node 2 or node 3 from node 1. We term this the "pre-deployment explosion' phenomenon.

Photonic agility, on the other hand, requires accurate nodal forecasts, as shown in Figure 1(c), since the photonic switch can direct any OEO from a nodal OEO pool to any direction and any lightpath. Thus, with the photonic agility only one OEO at the 1st node is required to provide the flexibility to connect it to either the 2nd or the 3rd node. The move from per-adjacency forecasts to nodal forecasts reduces the dependency on their accuracy and reduces the number of pre-deployed resources assuming imperfect forecasts. Even more importantly, it simplifies the planning process for the carrier, which in turn has a potential to further reduce the operational cost.

All of the factors described above translate into a different cost of the network for the different models of agility. To illustrate this, a comprehensive network study, using a real long-haul US network with real traffic demands, and based on real equipment costs was performed. The results of the study are shown in Fig. 2. The figure compares four network models: two manual networks - one with traffic growth but no churn (i.e., infinite connection lifetime) and the other with connection lifetimes of 6 months, electrical agility with a non-agile photonic layer and photonic agility. We did not include opaque networks since their cost was much higher than any of the other alternatives. For each model we detail the CAPEX costs and OPEX costs of labor and of delayed revenues. Since some of the costs are one-time CAPEX, while others are recurring OPEX, we use the "total cost of ownership" (TCO) to compare them, which we approximate by adding the CAPEX and the OPEX over a 5 year period and normalize based on the manual network without churn.

For each of the four options considered, the network was designed to accommodate two real-world traffic projections, A and B. The overall number of demands in A and B are the same, however 20% of the A-Zs (originations and terminations) are different. In the case of the manual scenarios, due to lack of remote agility, there is no need to pre-deploy resources, hence the OEOs are deployed as the traffic demand materializes. However, the OPEX due to manual visits and delayed revenues contribute to the TCO. For the electrical and photonic agility options, the network is designed and resources are pre-provisioned based on traffic pattern A. Then the network is presented demands from pattern B. If a particular demand cannot be satisfied through existing resources, additional resources, mainly OEOs and switching elements, are computed. At the end of this planning exercise, the network is capable to satisfy either of demand pattern A or B. From the economic analysis presented in Fig. 2, it is evident that a manually configured network is low cost if traffic stays for long periods of time. If the holding time of a connection is reduced, it

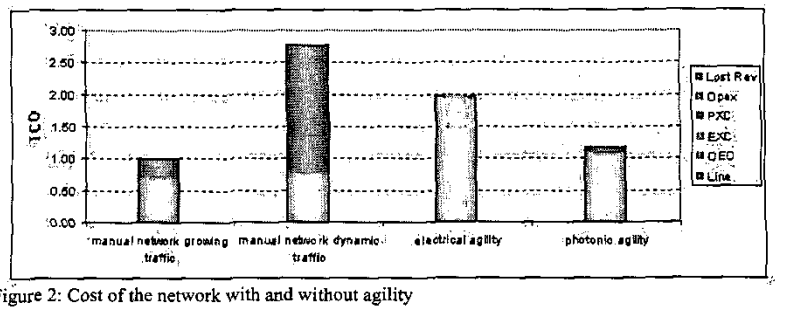

Figure 2: Cost of the network with and without agility